energies

MDPI

Review

A Short Review on Thermoelectric Glazing for Sustainable Built Environment

Mustafa Majid Rashak Al-Fartoos *, Anurag Roy, Tapas K. Mallick and Asif Ali Tahir *

Environment and Sustainability Institute, Faculty of Environment, Science and Economy, University of Exeter, Penryn Campus, Cornwall TR10 9FE, UK

* Correspondence: ma994@exeter.ac.uk (M.M.R.A.-F.); a.tahir@exeter.ac.uk (A.A.T.)

Abstract: Securing net-zero targets by employing sustainable materials for the built environment is highly desirable, and this can be achieved by retrofitting existing non-smart windows with thermoelectric (TE) glazing, providing improved thermal performance along with green electricity production. It is reported that TE glazing could produce ~4000 kWh of power per year in a cold climate with a temperature differential of ~22 °C. This feature of TE materials drives their emplacement as an alternative to existing glazing materials and could lead to the identification of optimum solutions for smart window development. However, few attempts have been made to employ TE materials in glazing. Therefore, in this brief review, we discuss, for the first time, the efforts made to employ TE in glazing, identify their drawbacks, and discuss potential solutions. Furthermore, the working principle, suitable materials, and methods for developing TE glazing are discussed. In addition, this article introduces a new research area and provides researchers with detailed instructions on how to build and optimize this system. The maximum efficiency of a thermoelectric material is determined by its thermoelectric figure of merit, which is a well-defined metric to characterize a device operating between the hot-side and cold-side temperatures. TE material's figure of merit promises new perspectives on the conceivable future energy-positive built environment. The role of TE in tackling the energy crisis is also discussed, since it provides sustainable energy alternatives

Keywords: building; figure of merit; glazing; material; thermoelectric

Citation: Al-Fartoos, M.M.R.; Roy, A.; Mallick, T.K.; Tahir, A.A. A Short Review on Thermoelectric Glazing for Sustainable Built Environment. *Energies* **2022**, *15*, 9589. https://doi.org/10.3390/en15249589

Academic Editor: Alessandro Cannavale

Received: 6 November 2022
Accepted: 14 December 2022
Published: 17 December 2022

1. Introduction

Climate change has increased the demand for research into reducing CO_2 emissions, which are the main reason for the current rapid climate changes. In the Paris Agreement, several countries have promised to reduce greenhouse gas emissions by making production and distribution more efficient, limiting carbon dioxide emissions from end users, and using more renewable energy sources to reach net zero by 2050 [1]. The United Kingdom (UK) became the first large economy in the world to enact a law requiring net-zero emissions in June 2019 [2]. This ambitious plan intends to cut the UK's net greenhouse gas emissions by 100% by 2050, compared with 1990 levels and replaces the UK's previous target from 2008 of reducing emissions by at least 80% [3]. Many innovative technologies can help to achieve this goal, such as photovoltaics; wind and water turbines; the production of clean hydrogen; caloric materials and batteries; green fuel; green steel; carbon capture; and energy saving technologies [4]. One of the required fields for reaching this aim is sustainable buildings. A sustainable building is any building that minimizes or eliminates harmful effects on our climate through its design, construction, and operation [5]. Several characteristics might make a building sustainable, such as sustainable eco-design; efficient energy consumption; using renewable energy; reducing pollution and waste energy; recycling; and utilising abundant, non-toxic materials [6]. In recent studies, it was found that buildings consume 20–40% of the total energy in developed countries [7], while studies in the UK show that at least 43% of total CO_2 emissions come from buildings, and 50% of energy consumption

is lost through building losses due to heating or air conditioning [8]. Therefore, it has become essential to develop building energy efficiency. In order to save waste energy, a glazing system should be employed, because the windows are considered the least energy-efficient part of buildings [9]. Buildings consume energy to create thermal and visual comfort, and transparent envelopes (windows and facades) are necessary to increase occupants' daylight, comfort, productivity, health, and well-being. Therefore, windows are considered an integral component of the built environment that is modelled to evaluate thermal transmittance to reduce the energy requirements of a whole building.

In the summer, most heat enters buildings through windows in the form of solar energy, which increases the energy consumption of air conditioning, while, during the winter, windows account for 30% of energy loss [7]. Energy-efficient glazing can reduce heat loss and, as a result, save money on bills by saving up to 145 pounds and 335 kg of carbon dioxide annually in the UK [10]. Glazings made with multilayer, vacuum, polymer-dispersed, thermochromic/electrochromic, low-emission, or phase change materials (PCMs) are still the most popular energy-saving glazing systems [11]. However, it is possible to save energy waste, harvest waste energy and convert it into electricity by implementing a thermoelectric generator (TEG) in glazing systems [12]. Thermoelectric (TE) materials are considered a clean and green energy conversion method since they can convert heat directly into electricity due to the Seebeck effect [13]. TE devices are easy to use, small, quiet, and require little maintenance because they have no moving parts [14,15]. The energy conversion efficiency of TE material depends on temperature differences and dimensionless figure-of-merit (ZT) TE material efficiency [16]. Some TE materials can produce electricity with only a 5 K temperature difference. For example, a bismuth telluride thermocouple can produce 5.5 μW at a 5 K temperature difference, reaching 100 μW at 100 K [17]. Likewise, it is possible to achieve 300 K temperature differences between outdoors and indoors in hot climates with the help of glazing, which increases the output of the TEG [11]. Moreover, the ZT is inversely proportional to thermal conductivity and directly proportional to the squared Seebeck coefficient (S) and the electrical conductivity (σ), which, together, make up the power factor ($PF = S^2\sigma$) [18].

Nevertheless, a ZT is temperature-dependent, and at least $ZT = 4$ is necessary to compete with other technologies, such as Rankine cycles, in terms of efficiency [19–21]. The ZT value of $Bi_{0.5}Sb_{1.5}Te_3$ can reach up to 1.86 at 320 K [22]. Therefore, combining glazing with TE increases isolation and reduces heat loss, leading to high TE efficiency and output power. For example, Inayat et al. (2014) produced 300 W from 9 m^2 thermoelectric glazing (TEGZ) with a temperature gradient of 20 °C; in a hot region with a temperature differential of 20 °C, TEGZ would produce 800 kWh of power per year on average. In a colder climate with a temperature differential of 22 °C during full-day operation, it would produce 3840 kWh of power per year [23]. These results signify that TEGZ is a potential energy-saving building envelope option in both hot and cold climates.

TEGZ has superiority over photovoltaics and solar thermal electricity in that it does not need a light source to work, can be functional at any time as long as there is a temperature gradient between indoors and outdoors, and, in addition, can use solar light to produce electricity. Figure 1 shows the working principle of TEGZ in hot and cold climates. In a hot climate, visible light is transmitted indoors while NIR light is absorbed by the outer surface and increases the outer surface temperature of the glazing. The indoor environment remains cold, as the insulation reflects most of the NIR light. In cold climates, the indoor heat is reflected by the insulation, which causes temperature differences. These temperature differences between indoor and outdoor environments produce electricity via mounted TEGs between the two glasses.

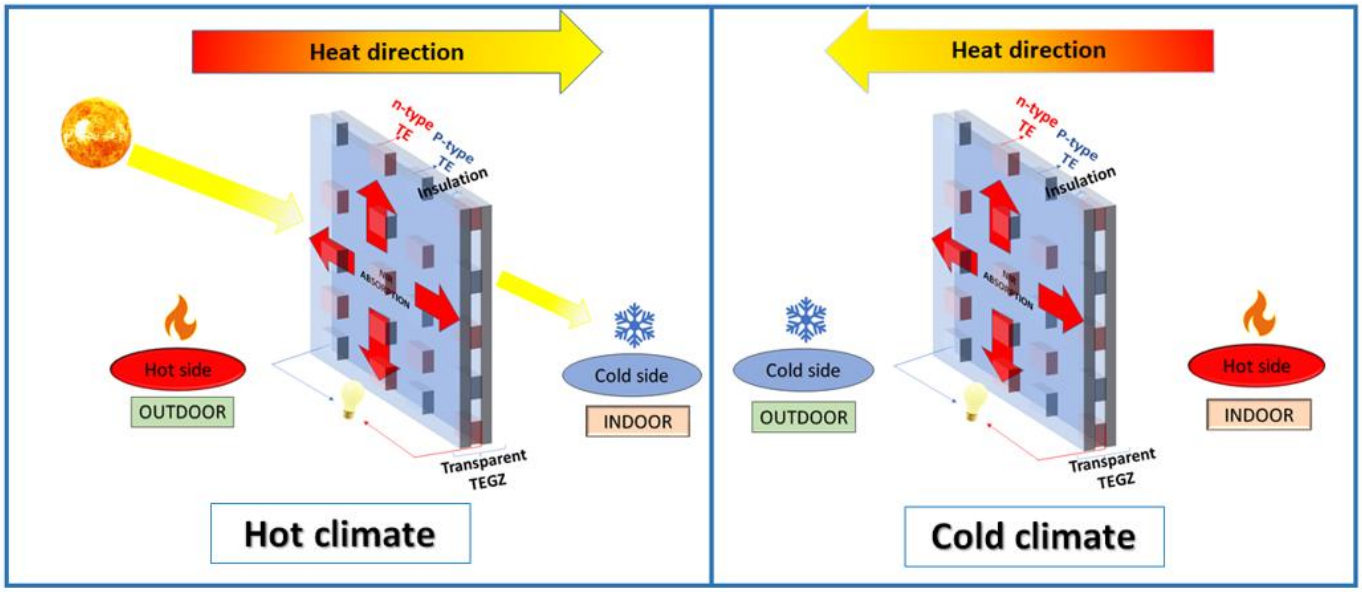

Figure 1. Glazing system working principle in hot and cold climates.

However, TE materials usually have poor efficiency, and TE materials with high-performance efficiency are costly to construct, highly toxic, made from rare earth elements, and non-transparent. In order to implement TE in glazing, TE's performance should be enhanced by increasing the *ZT*; fabrication of transparent, scalable, and cheap TE material from abundant earth elements; improving the glazing system (absorption and isolation); and developing a TE glazing modelling system, as illustrated in Figure 2. This review discusses TEGZ for the first time and highlights the attempts to fabricate TEGZ with an analysis of their drawbacks, the possible materials that could be used in TEGZ, and the path to optimize TEGZ.

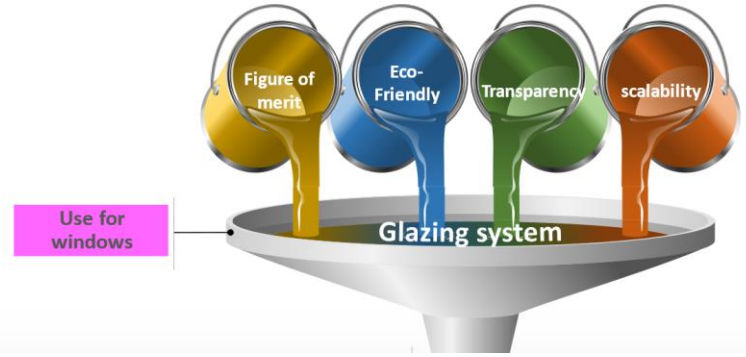

Figure 2. Schematic illustration of the areas to be focused on for developing TE glazing modeling.

2. Overview of Thermoelectricity

Working Principle

The Seebeck effect governs the working principle of the TEG. The Seebeck effect results when the junction of two dissimilar conductors or semiconductors is maintained under a temperature difference, enabling the charge carriers to move from the hot side to the cold side. This causes the charge to concentrate on the cold side, which leads to an induced potential that generates current when connected to circuits, as shown in (Figure 3) [15].

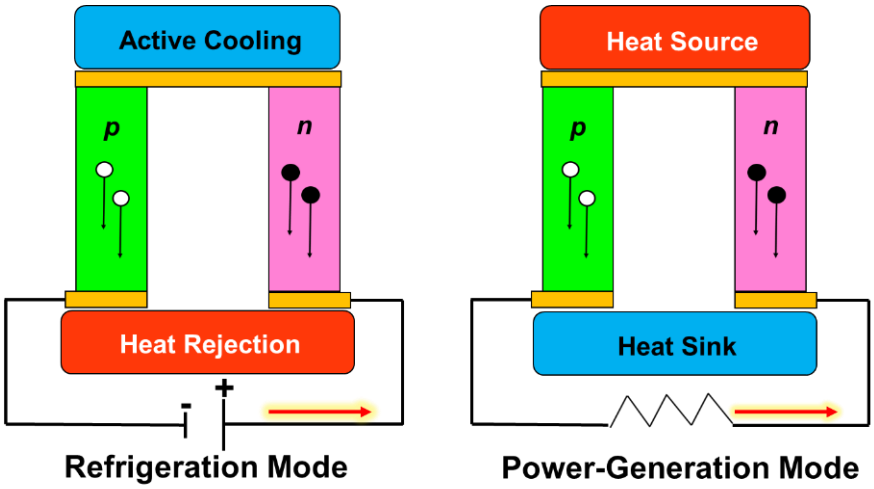

Figure 3. Working principle of TE materials in refrigeration and power generation modes.

In general, TE devices consist of p-type (most carriers are holes) and n-type (most carriers are electrons) semiconductors. TE material efficiency can be determined by using the ZT, which is given by the following Equation (1):

$$ZT = \frac{S^2\sigma}{K}T \tag{1}$$

where S, σ, k, and T are the Seebeck coefficient, the electrical conductivity, thermal conductivity, and absolute temperature, respectively [24]. Moreover, ZT influences the energy conversion efficiency of a TE device (η). Power generation efficiency is defined as the ratio of the electrical power output (W) to the thermal power provided (QH), as in the following Equation (2):

$$\eta = \mathrm{W/QH} = \frac{T_\mathrm{h} - T_\mathrm{c}}{T_\mathrm{h}} \times \frac{\sqrt{1+ZT}-1}{\sqrt{1+ZT}+\frac{T_\mathrm{c}}{T_\mathrm{h}}} \tag{2}$$

where (T_h) is the temperature on the hot side and (T_c) is the temperature on the cold side [13,15]. When the ZT approaches infinity, the efficiency approaches that of an optimum thermodynamic machine. This is because the ZT and efficiency are directly proportional. Furthermore, there must be a high Seebeck coefficient, high electrical conductivity, and low thermal conductivity to achieve a high ZT. The Seebeck coefficient (S) is primarily defined by the number of valence electrons that gain mobility from thermal energy input into the system and can be expressed by the equation below [15].

$$S = \Delta V/\Delta T \tag{3}$$

S is the Seebeck coefficient measured by μV/K, and V is the electrical voltage [15]. Several factors affect a material's Seebeck coefficient, including temperature and its chemical composition at a certain temperature [25]. In the case of electrons, electrical conductivity is given by:

$$\sigma = ne\mu \tag{4}$$

where n is the carrier density, e is the carrier charge, and μ is the carrier mobility [26]. Equation (4) shows that electrical conductivity can be increased by increasing the concentration and mobility, together or separately. The relationship between electrical conductivity and the Seebeck coefficient can be expressed by the power factor (PF) as the equation below [27]:

$$PF = S^2\sigma \tag{5}$$

There must be an immense power factor to achieve a high ZT. Thermal conductivity (k) is a material property that is made up of two parts: the phonon part of the lattice vibrations (k_l) and the electronic part (k_e).

$$k = k_e + k_l \tag{6}$$

Moreover, according to the Wiedemann–Franz relation below, high thermal conductivity in metals and degenerate semiconductors can be attributed to their electronic properties, as thermal conductivity is directly related to the electrical conductivity at a specified temperature [26,28].

$$k_e = L\sigma T = ne\mu LT \tag{7}$$

L is the Lorenz number (2.45×10^{-8} WΩk^{-2}) associated with a free electron. Since k_e relates to the Lorenz factor, which varies with the carrier concentration and transport method, it cannot be significantly altered apart from in low-carrier concentration materials, where the factor may be lowered by up to 20% of its free-electron value [16]. For the phonon part of the lattice, vibrations (k_l) can be expressed as the following:

$$k_l = \frac{1}{3} C_v l v_s \tag{8}$$

where C_v represents the specific heat at constant volume, l is the phonon mean free path, and v_s corresponds to the average velocity of sound [29]. A phonon is a quantum of vibrational energy in a material lattice that causes lattice thermal conductivity. It is possible to decrease the lattice thermal conductivity by increasing phonon scattering [16]. This is carried out in various approaches, such as porosity, alloying, nanostructuring, complex structures, etc.

From the above, it can be concluded that it is highly challenging to enhance the thermoelectric efficiency by increasing the ZT of TE materials because transport parameters (σ, S, and k) are interdependent. However, many methods can decouple these parameters, such as adjusting carrier concentrations, nanostructuring, phonon glass electron crystal (PGEC), etc.

3. Suitable Materials for Thermoelectric Glazing

TE can harvest heat energy in windows at low temperatures with a maximum temperature difference of 310 K. In addition; it can be produced on a large scale for a low cost, meaning that it can cover a large area of windows and easily be commercialized. Further, TE material should be transparent so that it does not affect indoor illumination. Moreover, non-toxic and abundant TE materials fit sustainability building requirements.

3.1. Low-Temperature Thermoelectric Materials

There is a wide range of TE materials, such as binary chalcogenides, clathrates, Zintl compounds, skutterudites, TE oxides, copper-based TE, polymer TE, etc., which can be divided into low-, medium-, and high-temperature TE. This is because the ZT is temperature-dependent, and no material can function reliably throughout an extensive temperature range since this affects its stability. The ZT peaks in most TE materials are bounded by the bipolar effect, which occurs because electron–hole pairs are created at a certain temperature during charge carrier excitation that can reduce the Seebeck coefficient and increase thermal conductivity. The rise in thermal conductivity and the drop in the Seebeck coefficient induced by the bipolar effect are almost diminished for band gaps more prominent than 10 k_BT. As a result, most high-temperature TE has high band gaps [30]. Semiconductors with band gaps of 0.26 eV are typically required for room-temperature TE materials [30,31]. Bismuth telluride, Zintl phase, and semiconductor polymers are promising candidates for using TE at room temperature.

A classic, effective TE material in low temperatures is Bismuth telluride (Bi_2Te_3), which is from the V–VI group of chalcogenide semiconductors [14]. Figure 4a shows the atomic arrangement in A_2B_3 (A = Bi, Sb; B = Se, Te, S) compounds. Bulk Bi_2Te_3 has a

rhombohedral crystal structure with the space group R3m, and its structure comprises the quintuple layers (QLs) of five atomic layers, Te-Bi-Te-Bi-Te, arranged in the c-direction [32]. Weak van der Waals forces separate the quintuple layers from one another [32]. Due to these weak bonds between subsequent quintuples, this compound has a layered structure, and the crystal can be readily fractured in this direction [16]. Several factors make this group of TE materials superior to all others. These compounds are highly anisotropic, with strong electrical conductivity, enhanced thermopower, an excellent Seebeck coefficient, and decreased thermal conductivity in the direction perpendicular to the c-direction, compared with the direction parallel to the c-direction [16]. Various methods can improve TE efficiency, including improving electronic transport characteristics, adjusting carrier concentration through doping, alloying, band structuring, and decreasing thermal conductivity by lowering the dimensions. A typical effective technique that has been used to enhance the TE performance of Bi_2Te_3 is dimensional reduction, such as via nanowires or superlattice thin film, while continuously controlling the transport characteristics to optimize the carrier concentrations. For example, p-type bismuth telluride was reported to have a high ZT = 1.41 at 300 K in bulk [32] and ZT = 1.80 at 316 K in nano dimensions [33]. The superlattices of Bi_2Te_3/Sb_2Te_3 improved the efficiency of $ZT > 2$ [34]. For n-type bismuth telluride, the maximum ZT = 1.1 at 300 K [32]. The p-type $Bi_{0.46}Te_{0.54}$ nanowires with a 100 nm diameter possess a Seebeck coefficient of 260 μVK^{-1} at 300 K, which is 60% greater than the $Bi_{0.46}Te_{0.54}$ bulk crystal [35]. Moreover, nanocomposites could be a powerful tool for improving TE properties [36]. For example, a ZT of n-type Bi_2Te_3 with 10 wt% nanocomposites increased by 43% compared with the bulk [37]. However, bismuth telluride is brittle and depends on rare earth elements, which are extremely rare, with only 0.001 ppm found in the earth's crust [38].

Zintl compounds are a new group of materials which show an attractive ZT[15,16,39]. Zintl phase, polar intermetallic compounds have attracted the attention of researchers because of their high TE efficiency, which is a result of their PGEC characteristics [16,40]. The Zintl compound phase offers a wide range of structural and chemical modifications, allowing significant changes to essential transport characteristics [15,16,39,41]. Moreover, complex structures of Zintl compounds result from the combination of ionic and covalent bonds. Ionic cations transfer electrons to covalently-bonded anions, resulting in a higher charge mobility than pure ionic materials [42]. Although they have excellent electrical conductivity, most Zintl compounds have relatively low thermal conductivity and high thermal stability at relatively high temperatures [16]. One of the most promising Zintl compounds at room temperature is Mg_3Sb_2. The crystal structure of $Mg_{3\times2}$ (X = Bi and Sb) is shown in Figure 4b. By using tantalum sealing, coarse-grained n-type $Mg_{3.05}Sb_{2-x-y}Bi_{y-x}Te_x$ ($x \leq 0.04$, $y \leq 1.5$) was synthesized and had a ZT of 0.7 at room temperature [43]. It is possible to enhance the TE performance of Mg_3Sb_2 by synthesizing a single crystal to increase its electrical conductivity. For example, Pan et al. (2020) achieved a ZT of 0.82 at 315 K in an n-type Y-doped $Mg_3Bi_{1.25}Sb_{0.75}$ single crystal [44]. Doping could be an effective method to increase performance. For example, Shi et al. (2019) synthesized Sc-doped Mg_3SbBi alloys with coarse grains and achieved a high ZT of 1.1 at 300–500 K using a melting and hot-deforming technique [45]. Band structure engineering could be a highly effective method for enhancing TE performance of materials by increasing the weighted mobility. For example, Han et al. (2020) enhanced the room-temperature TE performance of $Mg_{3+\delta}Sb_{2-y}Bi_y$ by increasing carrier mobility and achieved a ZT of 1.13 in the temperature range of 50–250 °C for $Mg_{3+\delta}Sb_{1.0}Bi_{1.0}$ [46].

Organic compounds have been exploited for electrical devices, such as electronics [47]. Recently, these materials have been used to create TE materials, which have promising applications for room temperature use due to their unique characteristics, such as low thermal conductivity; flexibility; lightweight and non-toxic properties; and ease of fabrication [25]. Organic materials, such as poly (3,4-ethylenedioxythiophene): poly (styrene sulfonate) (PEDOT: PSS); conducting polymers, such as polyaniline (PANI); non-conducting polymers, such as poly (3-octylthiophene); and organic semiconductors, such as pentacene, have all

been extensively studied for their TE characteristics and applications. Polymer materials, however, have low electrical conductivity, a low Seebeck coefficient, and a low power factor [48]. These limitations have been solved by developing organic polymer-inorganic TE composite materials which exhibit excellent TE performance [48]. Carbon nanotubes (CNTs) and graphene have been widely employed in fabricating organic TE materials to increase electrical conductivity. Lin et al. (2018) synthesised a p-phenediamino-modified graphene (PDG)/PANI composite for high-performance TE material, which achieved a *ZT* of 0.74 [49]. Recently, the high-record *ZT* = 0.75 for an ionic liquid/PEDOT: PSS heterostructure TE was achieved, which was attributed to a maximum two-fold increase in the Seebeck coefficient by the ionic liquid, which, surprisingly, did not impact electrical conductivity; this result is comparable to bismuth telluride (Bi_2Te_3) at 300 K [50].

The performance of flexible ternary polymer nanocomposite films has been enhanced by optimized interfacial architecture and results in high power factors of more than 500 $\mu W\ m^{-1}\ K^{-2}$. Moreover, ternary TE composites, such as the PEDOT: PSS/rGO (reduced graphene oxide)/Te nanowires (Te NWs), polypyrrole/graphene/PANI, and PEDOT: PSS/SWCNT/Te, have received a significant amount of attention due to the high TE performance that results from their unique internal structures and that increases the scattering at interfaces as well as the synergistic effect of their conductive components [26]. For example, the power factor of a ternary hybrid composite of PEDOT: PSS/rGO/Te NWs, as shown in Figure 4c, is 15 times higher than that of the binary film, which could be attributed to additional energy filtering at the interface between the rGO and PEDOT: PSS [51].

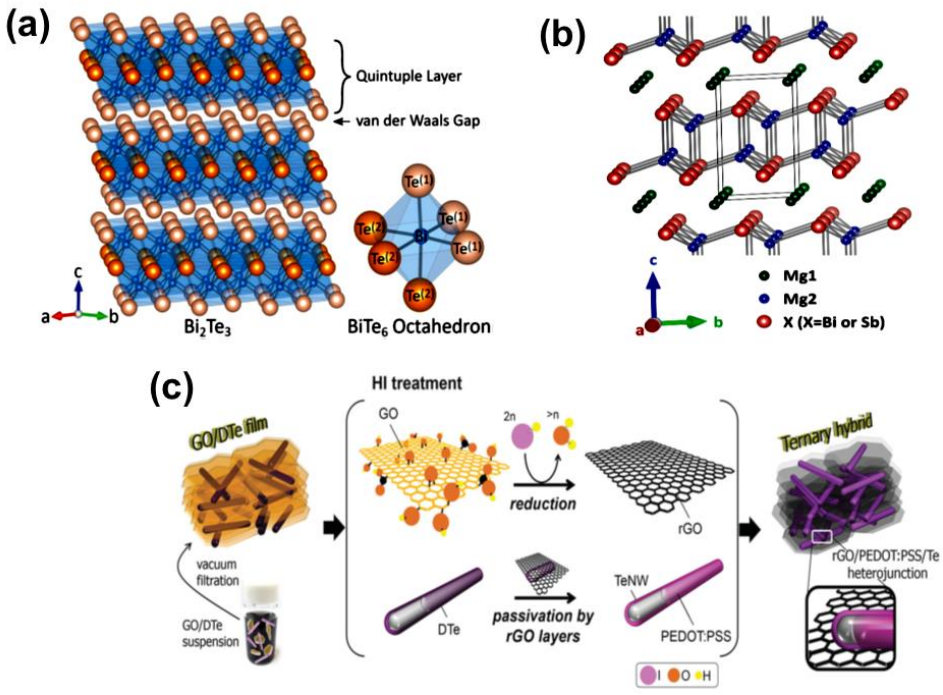

Figure 4. (**a**) Atomic structures of a bulk unit cell of Bi_2Te_3, adapted with permission from [14]. (**b**) Crystal structure of Mg_3X_2 system adapted with permission from [44]. (**c**) Schematic illustration of designed ternary TE composites adapted with permission from [51].

3.2. Transparent Thermoelectric Materials

Transparent conductive oxides, such as ZnO, have been intensively studied due to their high electrical conductivity, high transparency (over 80%), thermal durability at high temperatures, low toxicity, and low cost. The TE efficiency of ZnO can be increased by lowering the dimensions. For example, Ishibe et al. (2017) developed a highly-transparent embedded ZnO NWs where ZnO NWs, which possess high electrical conductivity and low thermal conductivity, were embedded in ZnO [52]. An exciting study showed that an

Sb-doped ZnO micro/nanobelt as a TE nanogenerator (TENG) produced an output voltage of 10 mV, an output current of 194 nA, and an output power of approximately 1.94 nW at a temperature gradient of 30 K [53]. The ZnO-based TE performance can be improved by doping, such as with Al, Ga, and Sb [54–57].

Another example of transparent TE conductive oxide is In_2O_3. Mo-doped bulk In_2O_3 improves TE performance, and a high *ZT* value of 0.75 at 1073 K has been reached [58]. Moreover, the nanoscale approach could be an excellent method to increase the TE performance of In_2O_3. At room temperature, indium tin oxide films with nanogranular structures have a low thermal conductivity of 0.84 $Wm^{-1}K^{-1}$ because of the increase in phonon scattering and a high-power factor of PF 3 $\mu W/mK^2$ at T = 300 °C, resulting in a roughly estimated *ZT* 1.9 for optimally-doped ITO films [59]. Gallium-doped In_2O_3: Sn (10%)-based multi-component metal oxides synthesized by spray pyrolysis show promising TE properties at 663 K, where the *ZT* was 0.26 [60]. Recently, transparent ITO/In_2O_3 thin films have been prepared by RF magnetron sputtering and show interesting TE properties [61–63].

Non-toxic and earth-abundant copper iodide (CuI) is a transparent and highly conductive p-type semiconductor that has gained recent interest for use in TE thin films due to its high TE performance at room temperature [64–66]. The pulsed laser deposition (PLD) technique is used to create highly transparent (90%) p-type γ-CuI thin films composed of fine nanoparticles with interesting TE properties at 300 K [66]. A transparent TE thin film made from CuI with a thickness of 300 nm has been fabricated, which recorded a maximum *ZT* value of 0.29 [67].

There are many other transparent conductive oxides (TCO) TE materials, such as SnO_2 [68–70] and CdO [71,72]. A recent theoretical study predicted that $BaSnO_3$ could be an excellent high-temperature TE, and that a *ZT* value of 2 at 1700 K might be reached [73].

In addition to organic-based TE materials' high mechanical flexibility, easy fabrication, lightweight properties, and ability to harvest heat at room temperature, they can also be transparent [74–76]. Flexible transparent TE prepared from the conducting polymer (PEDOT: PSS) as the p-type leg and (ITO)-PEDOT: PSS as the n-type leg shows excellent TE performance at room temperature, producing an output voltage of 3.1 mV from the temperature difference between human hands and the air alone [77]. High transparent (88.3%) and flexible TE nanofilms fabricated from a PEDOT: PSS thin film doped with DMSO/TSA and hydrazine/DMSO to optimize the oxidation level of PEDOT show a *ZT* of 0.31 at room temperature [78]. Transparent organic/inorganic multilayer films with a high-power factor of 110 W/mK^2 were created by alternately stacking PEDOT: PSS and PEDOT-SnSeTe nanosheets [79]. Other noteworthy materials are ionogels, which have recently attracted extensive attention as stretchable materials for wearable TE materials [80,81]. Wang et al. (2021) fabricated stretchable ionogels, via an in situ 3D printing method, with a thermomechanically and electrically stable performance over a wide range of temperatures [82].

3.3. Large-Scale Synthesis

The integration of TEGs into glazing requires large-scale TE synthesis and manufacturing processes to cover the large areas of windows. There are many options for the synthesis and fabrication of TE. However, many current synthesis techniques have drawbacks in terms of cost, construction time, complexity, mass production, scalability, and reliability [83]. Thus, finding an effective synthesis process that is easy to use, fast, cheap, high-quality, and scalable is crucial. For example, a large-scale screen-printing technique and a self-sustaining structure have been used to fabricate lightweight glass fabric-based flexible TEGs without top and bottom substrates and with a high output power density of (28 mWg^{-1} at 50 K temperature difference) [84]. Single-crystalline Bi_2Te_3 TE nanowires have been synthesized by chemical batch processing, converted into jettable ink, and then printed on a glass substrate, and this achieved a Seebeck coefficient of 140 μVK^{-1} [85]. Highly-crystalline ZnO films with a Seebeck coefficient of 36.6 μVK^{-1}-based micro-TE devices have been fabricated via electrodeposition, which consisted of four arrays; each

array had 55 pairs of TE elements with a 0.73 nW maximum of power generated [86]. Transparent CuI and ZnO films have been synthesized by low-temperature solution growth (SILAR), which allows for depositing the films over large areas to harvest near-infrared solar light energy [87].

4. Window Glazing

Glazing is a vital architectural component that enables visibility to connect with the outdoor environment, air ventilation, solar heating gain, and daylighting. However, since the U-values of windows are much higher than those of other building parts, they consume a large amount of energy. Building cooling and heating loads should be reduced to reduce carbon emissions, which is possible through increasing energy efficiency. Energy efficiency can be improved by reducing internal solar radiation and heat transmission from the inside to the outside in the winter. Thus, a growing desire exists to develop novel, high-performance glazing systems, such as smart composite-based transparent insulating materials, transparent infrared absorbers (TIA), and thermochromic materials (TCM).

4.1. Low Heat Gain Glazing

Double or triple glazing, low-emissivity coated glass, prismatic glazing, water- or air-flow glazing, vacuum glazing, and aerogel glazing are the most common methods for reducing solar heat gain through windows.

Air-filled double glazing is commonly used to reduce heat loss through windows [88]. It is possible to use other gases with a thermal conductivity lower than air, such as xenon, krypton, argon, and infrared radiation gas absorbers [89]. Moreover, the amount of heat lost by double glazing is proportional to the space between the panes of glass [89]. However, double glazing cannot control daylight and glare because of its high transparency. Prismatic glazing is an alternative method that can be used to control solar heat gain and generate uniform illumination without glare by redirecting or refracting sun rays [90]. Furthermore, water-flow glazing reduces solar heat gain into a building by lowering the temperature of glass panes via the flow of water between two panes and results in far superior energy saving than double windows [90]. However, it is highly costly to install water flow and pumping systems.

Vacuum glazing is a type of high-transmittance, thermally insulated glazing made up of two panes separated by a vacuum gap and held apart by a series of support pillars [91]. Vacuum glazing could lower heat loss by 53% compared with the same area of double glazing [92]. However, edge sealing directly affects thermal performance due to heat flowing from the glazing edge instead of the glass in vacuum glazing, which is known as the edge effect. The edge effect reduces thermal performance and increases stress on the edge, which can lead to glazing failure [93].

Aerogels are lightweight, low-density materials with a lower heat conductivity than air [94]. Silica aerogel is the most common type of aerogel, created by silica nanoparticles' aggregation [95]. However, aerogel glazing has several drawbacks, including slow synthesis and being fragile and expensive.

A low-emissivity (low-e) coating can minimize heat radiation from a glass surface [91]. Low-e coatings, which can be divided into hard and soft coatings, are spectrally selective metals or metallic oxides that allow visible light from the solar spectrum to pass through while blocking other wavelengths, such as infrared, which is responsible for heat gain [89]. Hard low-e coatings are more durable than soft low-e coatings because soft low-e coatings require additional layers of protection [93]. On the other hand, soft coatings have better infrared reflection and higher transparency [94]. The positioning of the coating is crucial for minimizing heat gain. Coatings on the outside glass surface cause most of the absorbed energy to reflect into the atmosphere outside rather than radiate back into the interior space, while low-e coatings placed on the inside surface of the interior glass pane lower heat loss from the interior space to the outer environment [88–90]. A hard coating, such as a pyrolytic coating, can be deposited directly onto the glass surface, while a soft coating,

usually consisting of multi-layered silver-based coatings, can be deposited by using MSVD techniques on hardened glass [96]. As much as 48% of solar heat gain can be blocked by low-e coatings on windows [97].

4.2. Smart Glazing

Smart glazing is an innovative technology that changes windows' visual and thermal transmittance properties to achieve the required degree of illumination or heating from solar radiation. There are, primarily, three types of intelligent windows: chromic windows (thermochromic, photochromic, and electrochromic), liquid crystal windows, and suspended particle devices [98]. The most promising innovations are electrochromic and suspended particle windows [99].

Electrochromic materials (whose optical properties change in response to electrical voltage or charge) for smart windows are the most reliable and up-and-coming technologies for controlling the optical properties of smart windows [97]. Absorbing electrochromic windows are already commercially available with efficient performance. Moreover, reflective electrochromic windows eliminate any heating difficulties that may arise from absorbing types and regulate more solar energy since they reflect solar radiation outside. However, electrochromic windows cannot provide total control over the uncomfortable effects of direct sunshine, such as glare and bright spots [97].

Thermochromic glazing is smart, non-electrically actuated glazing. When thermotropic materials' crystal structure changes due to heat, they undergo a physical phase shift when their critical temperature is surpassed, changing their radial properties and resulting in light scattering or absorption. Changing physical phases may result in losing some visible portions of the spectrum, limiting the view through a window. Figure 5a,b shows the structure of one type of thermochromic glazing and its transparency changes with temperature differences. Thermochromic materials can be inorganic or polymeric [96]. For example, one of the most promising alterable thermochromic materials is vanadium dioxide (VO_2), with a transition temperature (TC) of 68 °C, which behaves as an infrared-reflective metal above the TC. By contrast, below the TC, it behaves as an insulator and is infrared-transparent; these changes occur in 10-12 s [96,100]. Lei et al. (2022) developed a passive dual-control smart thermochromic window for energy savings by embedding poly (*N*-isopropylacrylamide) (PNIPAm) microgel within a highly transparent polyacrylamide (PAM) matrix. As a result, the window may lower the indoor air temperature by 15 °C [101].

Gasochromic glazing technology is active dynamic glazing for which the optical properties change to opaque when exposed to a low concentration of hydrogen and become transparent when exposed to oxygen [96,102,103]. A gasochromic film is composed of a highly porous transition metal oxide (WO_3, MoO_3, or V_2O_5) layer with a skinny coating of type catalyst (Pd or Pt nanoparticles) [96,102,103]. The solar heat gain coefficient for gasochromic materials ranges between 0.14 and 0.75 [97]. Single gasochromic panes have poor thermal insulation properties, and switching occurs by absorption rather than reflection, which leads to heating that develops into the overheating of interiors. To increase thermal performance, usually, gasochromic technology is combined with double- or triple-glazed units. Moreover, low-e coatings could be combined with a gasochromic pane.

Smart windows with humidity-chromic (HC) coatings are sensitive to humidity variations, allowing for adjustment of the amount of visible and infrared light coming in via a hydration and dehydration transition in the hydrogels [104,105]. A hydrogel is an aqueous polymer gel composed of water, hydrophilic polymers with hydrophobic groups, an amphipathic molecule, and sodium chloride [96,106]. Hydrogels are the phase transition materials used in switchable glazing because of their durability, adjustable chemical and physical characteristics, and acceptable switching speeds and mechanical strength [96,104,106]. Smart hydrogels have attracted attention as functional devices in several sectors, including coloring, self-cleaning, self-powering, and moisture absorption [104]. Hydrogels have several applications in smart window glazing, such as in thermochromic, electrochromic, photochromic, and HC coatings. Hydrogels have unique physical properties that can

respond to ambient humidity through water absorption/desorption and convert it to different signals, which can be used in smart window applications [96,104,106,107]. The scattering and transmittance of light in a hydrogel substance will vary depending on the relative humidity of the air in contact with the material; when the humidity is low, the light scattering is high, and some hydrogels become transparent, while others remain opaque [94,107]. There are two types of hydrogel responses: single (in which the response of the hydrogel to humidity is mainly reflected in its change in transparency and color) and dual (in which the hydrogel responds to the humidity and temperature sensitivity, or humidity and pH sensitivity) [104,107]. In addition to changes in light transmission and color, the reaction of hydrogels to humidity stimulation involves the production of electrical energy [104].

Polymer dispersed liquid crystal (PDLC) is electrically switchable glazing made of micro or nanometer droplets of liquid crystal (LC) held in a polymer matrix between two panes of glass [96,108,109]. Due to the random orientation of LC droplets in the polymer matrix, these films show a milky-white scattering condition, and once a sufficiently strong electric field is applied, the film becomes transparent; this is due to the alignment of LC droplets along the direction of the electric field, as shown in Figure 5c [96,108,109]. Switching a PDLC from the opaque to transparent mode takes around 1–40 ms when an electric voltage (about 2–10 V/μm) is applied [108]. PDLCs can be prepared using emulsion or phase separation techniques [108,109]. The conventional method of PDLC preparation, phase separation, enables precise control over the morphology and, consequently, the features of the finished film. This process can be initiated by heat action, solvent evaporation, or monomer polymerization. High-performance PDLC films used in smart glazing should have a high contrast ratio, a low threshold voltage, and a low switching time. Many factors influence the electro-optical properties of PDLC films, such as the type of phase separation method, the degree of phase separation, the size and morphology of the LC droplets, the exposure conditions, the film thickness, and the difference in the refractive index (RI) of the phases (LCs and polymer) [108,109].

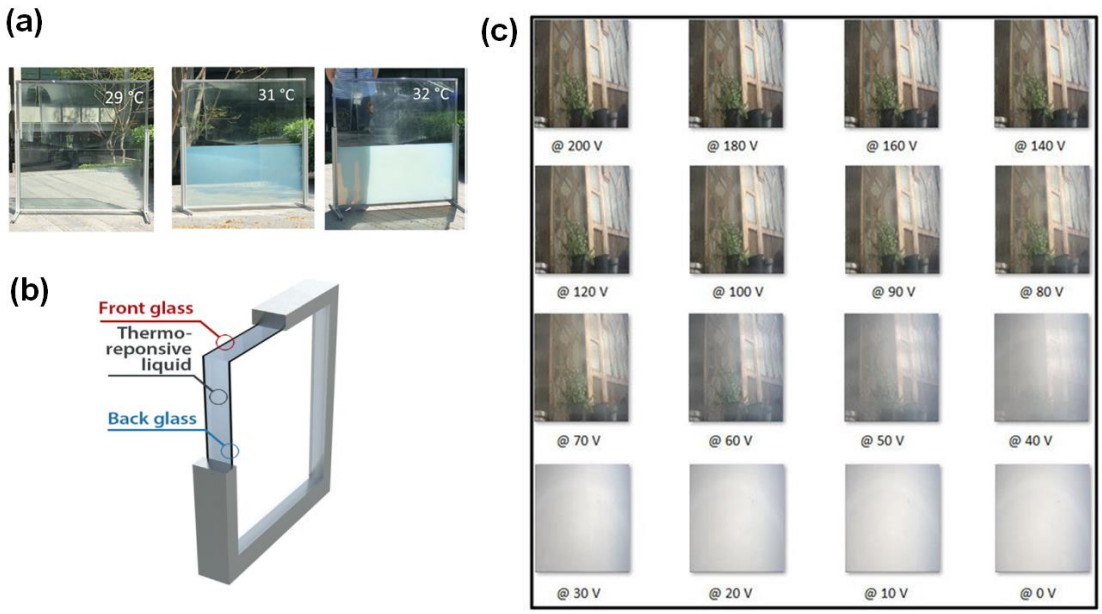

Figure 5. (**a**) Photograph of smart thermoresponsive glazing and corresponding transparencies tested at different temperatures. (**b**) Schematic illustration of the thermoresponsive glazed window adapted with permission from [9]. (**c**) PDLC glazing, for which transparency changes with applied voltages (V), is adapted with permission from [110].

5. Thermoelectric Glazing System

Recently, the exciting proposition of utilising TE in energy-efficient glazing has been raised. Energy-efficient glazing significantly reduces waste heat and makes houses warmer in winter and colder in summer by reducing heat transfer compared with ordinary glass, eventually reducing energy bills and the carbon footprint. Moreover, using energy-efficient glazing to increase sustainability is possible by employing TEGs, which simultaneously work as insulators and power generators. For example, Karimov et al. (2020) fabricated semi-transparent vertical cylinder-shaped TE cells with a transparency of 25%, based on bismuth antimony telluride alloy, that could be used to fabricate windows that may produce power [111]. They noticed that one layer of glass on the cells increased the light, heat, and open-circuit voltage. Increasing the pressure on the TE cylinders increased the conductivity and the maximum output of the power resulting from a high difference between the top and bottom surfaces when using a large receiver and water coolant [111].

It is crucial to fabricate transparent TE for utilization in glazing. For example, Yang et al. (2017) fabricated p-type transparent TE based on copper iodide (CuI) thin films (Figure 6a) with a high room-temperature performance. Their high TE performance is related to the low thermal conductivity of the CuI films, which is attributed to a combined effect of the heavy element iodine and strong phonon scattering, resulting in a prominent ZT = 0.21 at 300 K for the CuI films [112]. In another example, Wang et al. (2020) fabricated dense p-type PEDOT: PSS and the n-type indium tin oxide (ITO) counterpart thin film TE (Figure 6c), which showed ZT = 0.30 and 0.29 at 450 K and thermal conductivities of 0.22 and 0.32 $Wm^{-1}K^{-1}$, respectively. A TEG module with a high transmittance of >81% was fabricated using 10 pairs of dense p-type PEDOT: PSS and n-type ITO thin-film legs to produce 22.2 Wm^{-2} at a temperature gradient of 80 K [113].

To increase the efficiency of TEGZ, it is necessary to take advantage of the light by increasing the absorption of ultraviolet and infrared without reducing the transmission of light to increase the temperature difference. For example, Zhang et al. (2021) fabricated wavelength-selective film made of $Cs_{0.33}WO_3$ and resin, which had a high visible-light transmittance of up to 88% and enabled the efficient and selective harvesting of ultraviolet and infrared light, thereby converting absorbed light into heat without sacrificing transparency. A prototype that coupled the film with 12 Bi_2Te_3-based TEGs, as shown in Figure 6b, produced an extraordinary output voltage of ≈4 V within an area of 0.01 m^2 which was exposed to sunlight [114].

Likewise, TEGs implemented in glazing should have an efficient TE performance at room temperature to harvest more heat waste. For instance, He and colleagues (2020) created flexible amorphized $Ag_2Te_{1-x}S_x$-based glass TE materials with a high TE performance at room temperature, which is attributed to their ultra-low thermal conductivity. The Hall mobility of $Ag_2Te_{0.6}S_{0.4}$ is an order of magnitude greater than the best amorphous materials at room temperature, with an exceptional value of 750 $cm^2\ V^{-1}\ s^{-1}$ at a carrier concentration of $8.6 \times 10^{18}\ cm^{-3}$. At room temperature, the ZT was about 0.2 whereas, it reached to 0.7 at 575 K [115].

It is possible to increase the efficiency of TE glazing by optimizing the design of the glazing in conjunction with the latest technology used in glazing and the latest development in TE generation. For example, a finite element model (FEM) was created and tested by Dessel and Foubert (2010), as shown in Figure 6d, to ascertain the steady-state heat transfer for active thermal insulators (ATI) and to determine the ideal TE modules for this technology and the design of the double-glazing unit. They found that using the smallest, most closely-spaced TE modules yielded the most effective systems, and the design case produced the best results, including a vacuum cavity [116].

Solar TE could be used as an efficient tool to harvest waste heat in glazing. For example, He et al. (2018) fabricated a photo TE nanogenerator (PTENG) based on photothermal flexible and transferable film and a Te nanowire/PEDOT TE layer for harvesting environmental infrared (IR) light, as shown in Figure 6e. A potential difference may be created between two thin-film electrodes of silver paste deposited at each end of the film when the

device is illuminated by infrared light because of the photothermal effect and the Seebeck effect. By harvesting photothermal energy from sunlight at an atmospheric temperature of 20 °C, 10 thin-film PTENGs with dimensions of 1 cm x 3 cm each delivered an output voltage of 1.48 μV [117]. Moreover, Klochko et al. (2017) fabricated a semi-transparent solar TENG based on a pulsed electrodeposited array of ZnO nanorods on a transparent conducting fluorine-doped tin oxide (FTO) substrate, as shown in Figure 6f,g. This TENG operates due to a temperature difference between the 1-D ZnO array and the uncoated FTO, which is formed naturally when the ZnO/FTO mixture is heated by sunlight. At 50 °C, the NGs could produce 13 pW and, with optimum efficiency, they could reach up to 60 pW. A network of such TENGs composed of 32 semi-transparent ZnO/FTO solar TENGs can generate levels many times higher than a single TENG [12].

Furthermore, Norouzi et al. (2016) fabricated a TENG made of aluminium-doped zinc oxide (ZnO) nanorods synthesized by RF sputtering and growth via hydrothermal material on a glass substrate. For 1% Al-doped ZnO nanorods on the silicon substrate at a constant temperature difference of 1 K between the top and bottom of the nanorods, an open circuit voltage of 0.28 mV and an S.C current of 3.5 μA were obtained [118]. Ito et al. (2017) made thin-film TEGs using lithography and deposition processes with ball lenses that used chromatic aberration to separate visible and near-infrared (NIR) solar light, as shown in Figure 6h. The visible light which was transmitted was utilized as daylight, while the NIR light was employed for TE power. The 0.71 K difference in temperature between the p-n junctions on the surface of the TEG produced a maximum power of 51 $\mu W/m^2$ [119].

Conductive glasses are fascinating materials, including ITO [120], FTO [121], and chalcogenide glasses [122]. These glasses can be transparent TE materials and produced on a large scale, leading to their being implemented in glazing. For example, recently, Murmu et al. (2021) showed that phase separation and the improvement of TE properties in nanocomposite ITO films might be possible by tuning the oxygen partial pressure, which changes the oxygen concentration during deposition at room temperature [120].

TEGs embedded in windows could be a highly effective method for TE glazing. Inayat et al. (2012) fabricated window glass with 5-mm thickness embedded with four TE pellets made from ball-milled hot-pressed nanomaterials $_{(}Bi_{1.75}Te_{3.25)}$ and (Sb_2Te_3). The 5-mm glass helped maintain the temperature gradient of 23.5 °C between outdoors and indoors, resulting in a power of 0.112 μW [123]. Afterwards, Inayat fabricated a large (132.25 cm^2) Plexiglas panel and drilled 144 holes, which were integrated with 72 pairs of hot-pressed thermopiles made of $Bi_{0.4}Sb_{1.6}Te_3$ and $Bi_{1.75}Te_{3.25}$ nanopowders by mechanical alloying, as shown in Figure 6i. The resulting output of the panel was 0.16 μW for a temperature difference of 22.5 °C [23]. However, this high density of piles could reduce vision, leading to embedding TE in the window frame. For example, in one study, electrical energy was generated using 12 TEGs mounted in an aluminium window frame. The circuit was composed of 12 TEGs attached to a heat sink, a DCDC boost converter, and a power bank. A temperature difference of 16 °C between the air-conditioned room and the outside produced a maximum power of 0.61 watts [124]. However, TE embedded in the frame has only a small possible area for heat harvesting. Another design increases the visible area by embedding a 1μthick film of bismuth telluride and antimony telluride via PVD vertically through the 5 mm Plexiglas to produce 10 nW of thermopower generated by 21 °C temperature differences [125]. However, this method requires cutting the glass into strips and depositing the films in the side wall of the glass strip, which is a highly complicated, time-consuming, and expensive process. Table 1 illustrates recently attempted TEGZ system technologies, including those employing various TE materials.

Table 1. Summary of latest TGZ technologies.

No.	System	Transparency	Thermoelectric Performance	Isolation System	Absorption System	Complexity	Scalability for Large Area	Materials	Ref
1	Vertical cylinder-shaped TE cells	25% transparent	Voc more than 4000 μv at 60 ΔT	Coolant system	Uses one layer of glasses instead of multilayers	Complicated design	Difficult to fabricate on large scale	Depends on rare elements	[111]
2	Single leg, γ-CuI thin films	60–85% in the visible spectral range	ZT=0.21 at 300 K and power density of 2.4 mW cm^{-2} at ΔT = 50 K	-	-	Simple because it does not have isolation or absorption systems	Difficult to fabricate on large scale (sputtering)	Non-toxic and abundant earth elements	[112]
3	Transparent flexible thin-film p (PEDOT: PSS)–n (indium tin oxide) junction	81% transparent	ZT = 0.30 for p-type and 0.29 for n-type at 450 K and power density of 2220 mWcm^{-2} at 80 K	-	-	Simple	Difficult to fabricate on large scale (spin coating and sputtering)	Non-toxic and abundant earth elements	[113]
4	Absorbant glass coupled with TEG	88% transparent	The output voltage of ≈4 V within an area of 0.01 m^2	-	$Cs_{0.33}WO_3$ and resin	Simple	Large area of the glass can be covered for absorption by spray; however, it is difficult to scale TE material	Depends on rare elements	[114]
5	Active thermal isolator	-	It is an active thermal that produces heat rather than generating electricity	High isolation system by vacuum cavity	-	Complicated	Large area of the double-pane glass can be fabricated; however, it is difficult to scale TE material	Depends on rare elements	[116]
6	PTENG consisting of MoS2/PU photothermal film and Te/PEDOT TE layer	-	For area and at 20 °C temperature, the output voltage of 1.48 μV	The temperature difference arises from the horizontal distance between two thin-film electrodes	MoS_2/PU photothermal film for harvesting environmental infrared (IR) light	Complicated	Large-scale films can be fabricated but need multi steps	Depends on rare element (Te)	[117]
7	ZnO/FTO TENG	Semi-transparent	The maximum output power= 60 pW. At 50 20 °C Voc = 0.24 Mv Isc = 1.1 μA	-	1-D ZnO absorbs mid-infrared	Simple	Large-scale films can be fabricated by electrochemical deposition	Non-toxic and abundant earth elements	[12]
8	TEGs with ball lenses	The glass is transparent, but the TEGs and ball could be obstacles for the vision	The 0.71 K ΔT produces 51 μW/m^2	No	The NIR light can be harvested by chromatic aberrations induced by the small ball lenses.	Complicated	Difficult to fabricate on large scale	Depends on rare elements	[119]
9	Conductive glass (ITO)	75.4% transparent	The power factor = 17.3 μW $m^{-1}K^{-2}$	-	-	Simple	Can be produced on large scale	Non-toxic and abundant earth elements	[120]
10	Embedded TEGs in windows	The glass is transparent, but the TEGs are non-transparent, which limit vision	9 m^2 window can produce 300 W of power at 20 °C	-	-	Simple	It is difficult to scale the system for a large area as it needs multi steps; drill many holes to fabricate n-type and p-type nanomaterials, then fabricate the piles via hot press and connect the n-type with p-type	Depends on rare elements	[23]

We can conclude that it is crucial for emerging glazing and TE technologies to optimize the employment of TE in glazing. Moreover, it is recommended that future projects combine all the benefits of the attempts to produce low-cost and large-scale TE windows made from abundant eco-friendly materials with high heat absorption of ultraviolet and infrared radiation on the outdoor window surface and, at the same time, high isolation between the outdoors and indoors to increase temperature differences and reduce waste heat. Moreover, if the temperature differences between outdoors and indoors of 9 m^2 TEGZ remain constant at 22 °C throughout the year, the amount of electricity produced is approximately 4000 kWh, indicating that TEGZ is feasible [23]. Considering the global increase in electricity prices, with the price of electricity reaching 34 pence/kWh in the United Kingdom, TEGZ capital costs can be easily covered [126]. In addition, the average electricity consumption of a UK household is 2900 kWh per year, the same amount of power produced by TEGZ [25]. However, to produce this amount of electricity, users would need to maintain temperature differences between outdoors and indoors by using heating or air conditioning, which is not sustainable. Therefore, this concept offers a supplement to electric power from the main power grid, but it may not become the primary power source. Therefore, users do not need to keep their air conditioning or heating systems running to generate a temperature difference. This feature could only be used to power or charge small appliances when there is a natural difference in temperature. Further economic studies should be conducted to understand the feasibility of TEGZ in the presence of natural temperature differences.

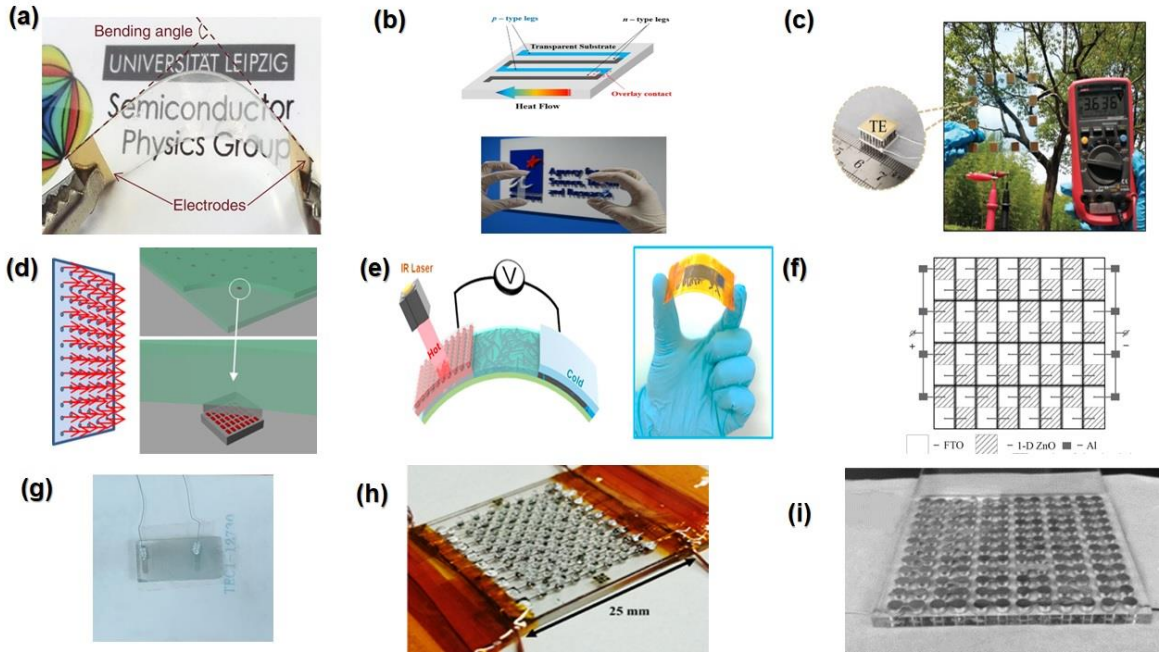

Figure 6. (**a**) Transparent flexible TE thin film made from CuI, adapted with permission from [112]. (**b**) Schematic representation of a basic configuration of p-type and n-type TE legs deposited on a substrate with a photo of the transparent TE device, adapted with permission from [113]. (**c**) Solar thermal electric power glass with 12 serially-connected Bi_2Te_3 TE modules, adapted with permission from [114]. (**d**) Active thermal insulator (ATI) glazing system, adapted with permission from [116]. (**e**) Schematic illustration of PTENG illuminated by an IR laser and an image of flexible PTENG, adapted with permission from [117]. (**f**, **g**) Photograph of a ZnO/FTO TENG with Al contact and schematic illustration of the proposed design for a network of semi-transparent ZnO/FTO solar TE NGs with Al contact adapted with permission from [12]. (**h**) TEG with ball lenses, adapted with permission from [119]. (**i**) TE glazing consisting of 144 holes integrated with 72 pairs, adapted with permission from [23].

6. Conclusions

Countries worldwide have agreed to reduce CO_2 emissions by using renewable energy sources to achieve net-zero emissions, which will reduce climate change. There are many methods to achieve this aim, such as photovoltaics, wind and water turbines, the production of clean hydrogen, etc. One area that can be effectively exploited to reach net zero is sustainable buildings. While windows are the primary source of natural light and indoor comfort, they are also the primary source of heat loss in buildings. In order to reduce energy consumption from windows, energy-efficient glazing should be used. There are many types of glazing to save energy, control lighting, etc. One of the notable types of glazing is thermoelectric glazing, which can reduce energy losses and produce electrical power that could be added to the grid.

The growing demand for clean energy and pollution reduction highlights the importance of TE. In particular, TE can reduce waste heat from general or even renewable energy sources. On the other hand, TE materials with high a power conversion efficiency are often either toxic or rare earth elements. Scientists have put great effort into developing high-efficiency TE eco-friendly materials. To employ TE in glazing, it is necessary to use high-performance transparent TE made from abundant, eco-friendly materials that can be easily fabricated for large-scale areas and to ensure their efficacy at room temperature.

There have been a few tentative attempts in this fascinating field. Recent efforts can be summarized as the implementation of TENGs in windows, the production of transparent TE, increasing the absorption of glass, the theoretical optimization of the design of glazing systems, the fabrication of flexible TE glass, and TE glass mass production. While these methods show the importance and effectiveness of TEGZ, they have many drawbacks, such as being expensive, complex, and toxic; however, it is possible to overcome these drawbacks in the future.

It is necessary to understand that TEGZ are a secondary source of power that can be added to the main grid. Therefore, there is no need to maintain the temperature difference between indoors and outdoors artificially.

7. Future Prospects

TEGZ are a fascinating and vital method to harvest waste heat energy from a building. However, to efficiently implement TE in glazing, systems should integrate efficient TE and glazing performance. To develop TE materials capable of being utilized in glazing, a continued effort must be made to manufacture non-toxic, earth-abundant TE to meet sustainability demands. More research should be conducted to make highly visible transparent TE materials for room temperature performance. Moreover, the focus should now be on how to fabricate and deposit these materials on large-scale areas to match the requirements of windows.

Materials such as bismuth telluride and zintl phase are notable for their low-temperature thermoelectric properties; however, they are opaque. Thus, the focus should be on increasing their transparency or developing TEGZ with a design that does not interfere with transparency and indoor comfort. Polymers and oxides, for example, are highly appealing due to their transparency; however, they have low efficiency, so the emphasis should be on increasing their efficiency.

Glazing systems with high ultraviolet and infrared radiation absorption surfaces should be developed to absorb the heat from solar radiation as much as possible. Moreover, high isolation performance between outer and inside surfaces should be achieved to increase the temperature difference, which could have a double effect on reducing heat waste and increasing TE performance. Furthermore, theoretical and modelling studies need to increase the efficiency of TE glazing system integration. Additionally, overall designs should be carefully studied to increase the waste heat harvesting output and efficiency of such systems. Finally, a further economic study should be held on the feasibility of TEGZ in the context of natural temperature differences.

Author Contributions: Conceptualization, methodology, writing-original draft preparation: M.M.R.A.-F.; RESOURCES, writing-review and editing: A.R.; supervision, writing—review and editing, project administration, funding acquisition: T.K.M. and A.A.T. All authors have read and agreed to the published version of the manuscript.

Funding: M.M.R.A.-F. acknowledges the Higher Committee of Education Development (HCED), Government of Iraq, for his PhD grant. A.R. and A.A.T. acknowledge the Engineering and Physical Sciences Research Council (EPSRC), UK, under research grant numbers EP/T025875/1 and EP/V049046/1. However, EPSRC was not directly involved in the writing of this article.

Data Availability Statement: Not applicable.

Conflicts of Interest: The authors declare no conflict of interest.

Nomenclature

Symbols	
C_v	Specific Heat at constant volume
*e*Isc	Carrier chargeshort circuit current
k	Thermal conductivity (W/m*K)
k_e	Electron thermal conductivity
k_l	Lattice thermal conductivity
L	Lorenz number
l	Phonons mean free path
n	Carrier density
QH	Thermal energy (hot side) (J)
S	Seebeck coefficient
T	Temperature (K)
T_c	The temperature on the cold side
T_h	The temperature on the hot side
*V*Voc	Voltage (V)The open circuit voltage
W	Power generated (W)
v_s	Average Sound velocity
σ	Electrical conductivity (S/m)
μ	Carrier mobility
Abbreviations	
ATI	Active thermal insulators
CNT	Carbon nanotube
HC	Humidity-chromic
FEM	Finite element model
NWs	Nanowires
PF	Power factor
PANI	Polyaniline
PEDOT: PSS	Poly(3,4-ethylenedioxythiophene): poly (styrene sulfonate)
PDLCPGEC	Polymer-dispersed liquid crystalsPhonon glass electron crystal
PTENGrGO	Photo-Thermoelectric NanogeneratorReduced graphene oxide
TCOs	Transparent conductive oxides
TCM	Thermochromic materials
TC	Transition temperature
TE	Thermo electric
TEGs	Thermoelectric generators
TEGZ	Thermoelectric glazing
TENG	Thermoelectric nanogenerator
TIA	Transparent infrared absorbers
SWCNT	Single-wall carbon nanotube
ZT	Figure of merit

References

1. The Paris Agreement. Available online: https://www.un.org/en/climatechange/paris-agreement (accessed on 4 September 2022).
2. UK Becomes First Major Economy to Pass Net Zero Emissions Law. Available online: https://www.gov.uk/government/news/uk-becomes-first-major-economy-to-pass-net-zero-emissions-law (accessed on 4 September 2022).
3. Climate Change Targets: The Road to Net Zero? Available online: https://lordslibrary.parliament.uk/climate-change-targets-the-road-to-net-zero/ (accessed on 4 September 2022).
4. Nieto, M. Whatever it Takes to Reach Net Zero Emissions around 2050 and Limit Global Warming to 1.5 c: The Cases of United States, China, European Union and Japan. *BAFFI CAREFIN Cent. Res. Pap.* **2022**, *170*, 1–25. [CrossRef]
5. John, G.; Clements-Croome, D.; Jeronimidis, G. Sustainable building solutions: A review of lessons from the natural world. *Build Environ.* **2005**, *40*, 319–328. [CrossRef]
6. GhaffarianHoseini, A.; Dahlan, N.D.; Berardi, U.; GhaffarianHoseini, A.; Makaremi, N.; GhaffarianHoseini, M. Sustainable energy performances of green buildings: A review of current theories, implementations and challenges. *Renew. Sustain. Energy Rev.* **2013**, *25*, 1–17. [CrossRef]
7. Hee, W.; Alghoul, M.; Bakhtyar, B.; Elayeb, O.; Shameri, M.; Alrubaih, M.; Sopian, K. The role of window glazing on daylighting and energy saving in buildings. *Renew. Sustain. Energy Rev.* **2015**, *42*, 323–343. [CrossRef]
8. Bahadori-Jahromi, A.; Rotimi, A.; Mylona, A.; Godfrey, P.; Cook, D. Impact of window films on the overall energy consumption of existing UK hotel buildings. *Sustainability* **2017**, *9*, 731. [CrossRef]
9. Zhou, Y.; Wang, S.; Peng, J.; Tan, Y.; Li, C.; Boey, F.Y.C.; Long, Y. Liquid Thermo-Responsive Smart Window Derived from Hydrogel. *Joule* **2020**, *4*, 2458–2474. [CrossRef]
10. Reducing Home Heat Loss Windows and Doors. Available online: https://energysavingtrust.org.uk/advice/windows-and-doors/ (accessed on 4 September 2022).
11. Roy, A.; Ullah, H.; Alzahrani, M.; Ghosh, A.; Mallick, T.K.; Tahir, A.A. Synergistic Effect of Paraffin-Incorporated In2O3/ZnO Multifold Smart Glazing Composite for the Self-Cleaning and Energy-Saving Built Environment. *ACS Sustain. Chem. Eng.* **2022**, *10*, 6609–6621. [CrossRef]
12. Klochko, N.; Klepikova, K.; Kopach, V.; Tyukhov, I.; Starikov, V.; Sofronov, D.; Khrypunova, I.; Zhadan, D.; Petrushenko, S.; Dukarov, S. Development of semi-transparent ZnO/FTO solar thermoelectric nanogenerator for energy efficient glazing. *Sol. Energy* **2019**, *184*, 230–239. [CrossRef]
13. Mamur, H.; Dilmaç, Ö.F.; Begum, J.; Bhuiyan, M.R.A. Thermoelectric generators act as renewable energy sources. *Cleaner Materials* **2021**, *2*, 100030. [CrossRef]
14. Witting, I.T.; Chasapis, T.C.; Ricci, F.; Peters, M.; Heinz, N.A.; Hautier, G.; Snyder, G.J. The thermoelectric properties of bismuth telluride. *Adv. Electron. Mater.* **2019**, *5*, 1800904. [CrossRef]
15. Rowe, D.M. *Thermoelectrics Handbook: Macro to Nano*; CRC Press: Boca Raton, FL, USA, 2006; ISBN 1315220393.
16. Ravindra, N.; Jariwala, B.; Bañobre, A.; Maske, A. *Thermoelectrics: Fundamentals, Materials Selection, Properties, and Performance*; Springer: Cham, Switzerland, 2018; ISBN 3319963414.
17. El Oualid, S.; Kosior, F.; Dauscher, A.; Candolfi, C.; Span, G.; Mehmedovic, E.; Paris, J.; Lenoir, B. Innovative design of bismuth-telluride-based thermoelectric micro-generators with high output power. *Energy Environ. Sci.* **2020**, *13*, 3579–3591. [CrossRef]
18. Poudel, B.; Hao, Q.; Ma, Y.; Lan, Y.; Minnich, A.; Yu, B.; Yan, X.; Wang, D.; Muto, A.; Vashaee, D.; et al. High-Thermoelectric Performance of Nanostructured Bismuth Antimony Telluride Bulk Alloys. *Science* **2008**, *320*, 634–638. [CrossRef] [PubMed]
19. Biswas, K.; He, J.; Blum, I.D.; Wu, C.I.; Hogan, T.P.; Seidman, D.N.; Dravid, V.P.; Kanatzidis, M.G. High-performance bulk thermoelectrics with all-scale hierarchical architectures. *Nature* **2012**, *489*, 414–418. [CrossRef]
20. Vining, C.B. An inconvenient truth about thermoelectrics. *Nat. Mater.* **2009**, *8*, 83–85. [CrossRef]
21. Shakouri, A. Recent developments in semiconductor thermoelectric physics and materials. *Annu. Rev. Mater. Res.* **2011**, *41*, 399–431. [CrossRef]
22. Kim, E.B.; Dharmaiah, P.; Lee, K.-H.; Lee, C.-H.; Lee, J.-H.; Yang, J.-K.; Jang, D.-H.; Kim, D.-S.; Hong, S.-J. Enhanced thermoelectric properties of Bi0. 5Sb1. 5Te3 composites with in-situ formed senarmontite Sb2O3 nanophase. *J. Alloys. Compd.* **2019**, *777*, 703–711. [CrossRef]
23. Inayat, S.B.; Rader, K.R.; Hussain, M.M. Manufacturing of Thermoelectric Nanomaterials (Bi0. 4Sb1. 6Te3/Bi1. 75Te3. 25) and Integration into Window Glasses for Thermoelectricity Generation. *Energy Technol.* **2014**, *2*, 292–299. [CrossRef]
24. Zulkepli, N.; Yunas, J.; Mohamed, M.A.; Hamzah, A.A. Review of Thermoelectric Generators at Low Operating Temperatures: Working Principles and Materials. *Micromachines* **2021**, *12*, 734. [CrossRef] [PubMed]
25. Zhang, Y.; Heo, Y.-J.; Park, M.; Park, S.-J. Recent advances in organic thermoelectric materials: Principle mechanisms and emerging carbon-based green energy materials. *Polymers* **2019**, *11*, 167. [CrossRef]
26. Snyder, G.J.; Toberer, E.S. Complex thermoelectric materials. *Nat. Mater.* **2008**, *7*, 105–114. [CrossRef]
27. Li, A.; Hu, C.; He, B.; Yao, M.; Fu, C.; Wang, Y.; Zhao, X.; Felser, C.; Zhu, T. Demonstration of valley anisotropy utilized to enhance the thermoelectric power factor. *Nat. Commun.* **2021**, *12*, 1–9. [CrossRef] [PubMed]
28. Zakharchuk, K.V.; Tobaldi, D.M.; Xiao, X.; Xie, W.; Mikhalev, S.M.; Martins, J.F.; Frade, J.R.; Weidenkaff, A.; Kovalevsky, A.V. Synergistic effects of zirconium-and aluminum co-doping on the thermoelectric performance of zinc oxide. *J. Eur. Ceram. Soc.* **2019**, *39*, 1222–1229. [CrossRef]

29. Sootsman, J.R.; Chung, D.Y.; Kanatzidis, M.G. New and old concepts in thermoelectric materials. *Angew. Chem. Int. Ed.* **2009**, *48*, 8616–8639. [CrossRef] [PubMed]
30. Han, Z.; Li, J.-W.; Jiang, F.; Xia, J.; Zhang, B.-P.; Li, J.-F.; Liu, W. Room-temperature thermoelectric materials: Challenges and a new paradigm. *J. Materiomics.* **2022**, *8*, 427–436. [CrossRef]
31. Li, A.; Fu, C.; Zhao, X.; Zhu, T. High-Performance Mg3Sb2-x Bi x Thermoelectrics: Progress and Perspective. *Research* **2020**, *2020*, 1934848. [CrossRef] [PubMed]
32. Zahid, F.; Lake, R. Thermoelectric properties of Bi_2 Te_3 atomic quintuple thin films. *Appl. Phys. Lett.* **2010**, *97*, 212102. [CrossRef]
33. Fan, S.; Zhao, J.; Guo, J.; Yan, Q.; Ma, J.; Hng, H.H. p-type $Bi_{0.4}$ $Sb_{1.6}$ Te_3 nanocomposites with enhanced figure of merit. *Appl. Phys. Lett.* **2010**, *96*, 182104. [CrossRef]
34. Venkatasubramanian, R.; Siivola, E.; Colpitts, T.; O'Quinn, B. Thin-film thermoelectric devices with high room-temperature figures of merit. *Nature* **2001**, *413*, 597–602. [CrossRef]
35. Zhou, J.; Jin, C.; Seol, J.H.; Li, X.; Shi, L. Thermoelectric properties of individual electrodeposited bismuth telluride nanowires. *Appl. Phys. Lett.* **2005**, *87*, 133109. [CrossRef]
36. El-Makaty, F.M.; Ahmed, H.K.; Youssef, K.M. Review: The effect of different nanofiller materials on the thermoelectric behavior of bismuth telluride. *Mater. Des.* **2021**, *209*, 109974. [CrossRef]
37. Fan, S.; Zhao, J.; Yan, Q.; Ma, J.; Hng, H.H. Influence of nanoinclusions on thermoelectric properties of n-type Bi2Te3 nanocomposites. *J. Electron. Mater.* **2011**, *40*, 1018–1023. [CrossRef]
38. Amatya, R.; Ram, R. Trend for thermoelectric materials and their earth abundance. *J. Electron. Mater.* **2012**, *41*, 1011–1019. [CrossRef]
39. Chen, L.; Liu, R.; Shi, X. *Thermoelectric Materials and Devices*; Elsevier: Amsterdam, The Netherlands, 2020; ISBN 0128184140.
40. Kauzlarich, S.M.; Zevalkink, A.; Toberer, E.; Snyder, G.J. Chapter 1 Zintl Phases: Recent Developments in Thermoelectrics and Future Outlook. In *Thermoelectric Materials and Devices*; Iris Nandhakumar, N.M.W., Stephen, B., Eds.; The Royal Society of Chemistry: Cambridge, UK, 2017; pp. 1–26. ISBN 2044-0774.
41. Toberer, E.S.; May, A.F.; Snyder, G.J. Zintl Chemistry for Designing High Efficiency Thermoelectric Materials. *Chem. Mater.* **2010**, *22*, 624–634. [CrossRef]
42. Mulla, R.; Rabinal, M.H.K. Copper sulfides: Earth-abundant and low-cost thermoelectric materials. *Energy Technol.* **2019**, *7*, 1800850. [CrossRef]
43. Shi, X.; Sun, C.; Bu, Z.; Zhang, X.; Wu, Y.; Lin, S.; Li, W.; Faghaninia, A.; Jain, A.; Pei, Y. Revelation of Inherently High Mobility Enables Mg3Sb2 as a Sustainable Alternative to n-Bi2Te3 Thermoelectrics. *Adv. Sci.* **2019**, *6*, 1802286. [CrossRef]
44. Pan, Y.; Yao, M.; Hong, X.; Zhu, Y.; Fan, F.; Imasato, K.; He, Y.; Hess, C.; Fink, J.; Yang, J. Mg 3 (Bi, Sb) 2 single crystals towards high thermoelectric performance. *Energy Environ. Sci.* **2020**, *13*, 1717–1724. [CrossRef]
45. Shi, X.; Sun, C.; Zhang, X.; Chen, Z.; Lin, S.; Li, W.; Pei, Y. Efficient Sc-Doped $Mg_{3.05-x}Sc_xSbBi$ Thermoelectrics Near Room Temperature. *Chem. Mater.* **2019**, *31*, 8987–8994. [CrossRef]
46. Han, Z.; Gui, Z.; Zhu, Y.B.; Qin, P.; Zhang, B.-P.; Zhang, W.; Huang, L.; Liu, W. The Electronic Transport Channel Protection and Tuning in Real Space to Boost the Thermoelectric Performance of Mg3+δSb2-yBiy near Room Temperature. *Research* **2020**, *2020*, 1672051. [CrossRef]
47. Barink, M.; Van den Berg, D.; Yakimets, I.; Giesen, P.; Van Dommelen, J.A.; Meinders, E. Flexible electronics: Prediction of substrate deformation during different steps of the lithography process. *Microelectron. Eng.* **2011**, *88*, 999–1005. [CrossRef]
48. Du, Y.; Shen, S.Z.; Cai, K.; Casey, P.S. Research progress on polymer–inorganic thermoelectric nanocomposite materials. *Prog. Polym. Sci.* **2012**, *37*, 820–841. [CrossRef]
49. Lin, Y.-H.; Lee, T.-C.; Hsiao, Y.-S.; Lin, W.-K.; Whang, W.-T.; Chen, C.-H. Facile Synthesis of Diamino-Modified Graphene/Polyaniline Semi-Interpenetrating Networks with Practical High Thermoelectric Performance. *ACS Appl. Mater. Interfaces* **2018**, *10*, 4946–4952. [CrossRef] [PubMed]
50. Fan, Z.; Du, D.; Guan, X.; Ouyang, J. Polymer films with ultrahigh thermoelectric properties arising from significant seebeck coefficient enhancement by ion accumulation on surface. *Nano Energy* **2018**, *51*, 481–488. [CrossRef]
51. Choi, J.; Lee, J.Y.; Lee, S.S.; Park, C.R.; Kim, H. High-performance thermoelectric paper based on double carrier-filtering processes at nanowire heterojunctions. *Adv. Energy Mater.* **2016**, *6*, 1502181. [CrossRef]
52. Ishibe, T.; Tomeda, A.; Watanabe, K.; Kikkawa, J.; Fujita, T.; Nakamura, Y. Embedded-ZnO Nanowire Structure for High-Performance Transparent Thermoelectric Materials. *J. Electron. Mater.* **2017**, *46*, 3020–3024. [CrossRef]
53. Yang, Y.; Pradel, K.C.; Jing, Q.; Wu, J.M.; Zhang, F.; Zhou, Y.; Zhang, Y.; Wang, Z.L. Thermoelectric nanogenerators based on single Sb-doped ZnO micro/nanobelts. *ACS Nano* **2012**, *6*, 6984–6989. [CrossRef]
54. Jood, P.; Mehta, R.J.; Zhang, Y.; Peleckis, G.; Wang, X.; Siegel, R.W.; Borca-Tasciuc, T.; Dou, S.X.; Ramanath, G. Al-doped zinc oxide nanocomposites with enhanced thermoelectric properties. *Nano Lett.* **2011**, *11*, 4337–4342. [CrossRef]
55. Tomeda, A.; Ishibe, T.; Taniguchi, T.; Okuhata, R.; Watanabe, K.; Nakamura, Y. Enhanced thermoelectric performance of Ga-doped ZnO film by controlling crystal quality for transparent thermoelectric films. *Thin Solid Film.* **2018**, *666*, 185–190. [CrossRef]
56. Pham, A.T.T.; Le, O.K.T.; Phan, T.T.T.; Van Hoang, D.; Nguyen, T.H.; Le, N.D.; Phan, T.B.; Tran, V.C. Enhancing transparent thermoelectric properties of Sb-doped ZnO thin films via controlled deposition temperature. *Vacuum* **2022**, *202*, 111137. [CrossRef]
57. Wang, X.; Huang, X.; Wong, Z.M.; Suwardi, A.; Zheng, Y.; Wei, F.; Wang, S.; Tan, T.L.; Wu, G.; Zhu, Q. Gallium-Doped Zinc Oxide Nanostructures for Tunable Transparent Thermoelectric Films. *ACS Appl. Nano Mater.* **2022**, *5*, 8631–8639. [CrossRef]

58. Klich, W.; Ohtaki, M. Thermoelectric properties of Mo-doped bulk In2O3 and prediction of its maximum. *ZT Ceram. Int.* **2021**, *47*, 18116–18121. [CrossRef]
59. Brinzari, V.I.; Cocemasov, A.I.; Nika, D.L.; Korotcenkov, G.S. Ultra-low thermal conductivity of nanogranular indium tin oxide films deposited by spray pyrolysis. *Appl. Phys. Lett.* **2017**, *110*, 071904. [CrossRef]
60. Korotcenkov, G.; Brinzari, V.; Cho, B. In2O3-based multicomponent metal oxide films and their prospects for thermoelectric applications. *Solid State Sci.* **2016**, *52*, 141–148. [CrossRef]
61. Tchenka, A.; Agdad, A.; Mellalou, A.; Chaik, M.; el Haj, D.A.; Narjis, A.; Nkhaili, L.; Ibnouelghazi, E.; Ech-Chamikh, E. Spectroscopic Investigations and Thermoelectric Properties of RF-Sputtered ITO Thin Films. *J. Electron. Mater.* **2022**, *51*, 1401–1408. [CrossRef]
62. Zhang, J.; Wang, W.; Liu, D.; Zhang, Y.; Shi, P. Structural and electric response of ITO/In2O3 transparent thin film thermocouples derived from RF sputtering at room temperature. *J. Mater. Sci. Mater. Electron.* **2018**, *29*, 20253–20259. [CrossRef]
63. Shi, Z.; Zhang, J.; Wang, W.; Zhang, Y.; Chen, B.; Shi, P. Effect of SiO2 buffer layer on thermoelectric response of In2O3/ITO thin film thermocouples. *J. Alloys. Compd.* **2022**, *902*, 163838. [CrossRef]
64. Klochko, N.P.; Barbash, V.A.; Klepikova, K.S.; Kopach, V.R.; Tyukhov, I.I.; Yashchenko, O.V.; Zhadan, D.O.; Petrushenko, S.I.; Dukarov, S.V.; Lyubov, V.M.; et al. Use of biomass for a development of nanocellulose-based biodegradable flexible thin film thermoelectric material. *Sol. Energy* **2020**, *201*, 21–27. [CrossRef]
65. Klochko, N.P.; Zhadan, D.O.; Klepikova, K.S.; Petrushenko, S.I.; Kopach, V.R.; Khrypunov, G.S.; Lyubov, V.M.; Dukarov, S.V.; Khrypunova, A.L. Semi-transparent copper iodide thin films on flexible substrates as p-type thermolegs for a wearable thermoelectric generator. *Thin Solid Film.* **2019**, *683*, 34–41. [CrossRef]
66. Klochko, N.P.; Kopach, V.R.; Tyukhov, I.I.; Khrypunov, G.S.; Korsun, V.E.; Nikitin, V.O.; Lyubov, V.M.; Kirichenko, M.V.; Otchenashko, O.N.; Zhadan, D.O.; et al. Wet chemical synthesis of nanostructured semiconductor layers for thin-film solar thermoelectric generator. *Sol. Energy* **2017**, *157*, 657–666. [CrossRef]
67. Coroa, J.; Morais Faustino, B.M.; Marques, A.; Bianchi, C.; Koskinen, T.; Juntunen, T.; Tittonen, I.; Ferreira, I. Highly transparent copper iodide thin film thermoelectric generator on a flexible substrate. *RSC Adv.* **2019**, *9*, 35384–35391. [CrossRef]
68. Khademi, N.; Bagheri-Mohagheghi, M.; Shirpay, A. Bi-doped SnO2 transparent conducting thin films deposited by spray pyrolysis: Structural, electrical, optical, and photo-thermoelectric properties. *Opt. Quant. Electron.* **2022**, *54*, 130. [CrossRef]
69. Bagheri-Mohagheghi, M.-M.; Shahtahmasebi, N.; Alinejad, M.R.; Youssefi, A.; Shokooh-Saremi, M. Fe-doped SnO2 transparent semi-conducting thin films deposited by spray pyrolysis technique: Thermoelectric and p-type conductivity properties. *Solid State Sci.* **2009**, *11*, 233–239. [CrossRef]
70. Ferreira, M.; Loureiro, J.; Nogueira, A.; Rodrigues, A.; Martins, R.; Ferreira, I. SnO2 thin film oxides produced by rf sputtering for transparent thermoelectric devices. *Mater. Today Proc.* **2015**, *2*, 647–653. [CrossRef]
71. Gao, L.; Wang, S.; Liu, R.; Zhai, S.; Zhang, H.; Wang, J.; Fu, G. The effect of Ni doping on the thermoelectric transport properties of CdO ceramics. *J. Alloy. Compd.* **2016**, *662*, 213–219. [CrossRef]
72. Saha, B.; Thapa, R.; Chattopadhyay, K.K. Improvement of electrical and thermoelectric properties of CdO thin film by aluminum doping. In Proceedings of the International Workshop on Physics of Semiconductor Devices, Mumbai, India, 16–20 December 2007; pp. 423–426. [CrossRef]
73. Spooner, K.B.; Ganose, A.M.; Scanlon, D.O. Assessing the limitations of transparent conducting oxides as thermoelectrics. *J. Mater. Chem. A* **2020**, *8*, 11948–11957. [CrossRef]
74. Ponder, J.F., Jr.; Menon, A.K.; Dasari, R.R.; Pittelli, S.L.; Thorley, K.J.; Yee, S.K.; Marder, S.R.; Reynolds, J.R. Conductive, Solution-Processed Dioxythiophene Copolymers for Thermoelectric and Transparent Electrode Applications. *Adv. Energy Mater.* **2019**, *9*, 1900395. [CrossRef]
75. Park, C.; Yoo, D.; Im, S.; Kim, S.; Cho, W.; Ryu, J.; Kim, J.H. Large-scalable RTCVD Graphene/PEDOT: PSS hybrid conductive film for application in transparent and flexible thermoelectric nanogenerators. *RSC Adv.* **2017**, *7*, 25237–25243. [CrossRef]
76. Yang, Y.; Deng, H.; Fu, Q. Recent progress on PEDOT: PSS based polymer blends and composites for flexible electronics and thermoelectric devices. *Mater. Chem. Front.* **2020**, *4*, 3130–3152. [CrossRef]
77. Dong, X.; Xiong, S.; Luo, B.; Ge, R.; Li, Z.; Li, J.; Zhou, Y. Flexible and Transparent Organic–Inorganic Hybrid Thermoelectric Modules. *ACS Appl. Mater. Interfaces* **2018**, *10*, 26687–26693. [CrossRef]
78. Lee, S.H.; Park, H.; Kim, S.; Son, W.; Cheong, I.W.; Kim, J.H. Transparent and flexible organic semiconductor nanofilms with enhanced thermoelectric efficiency. *J. Mater. Chem. A* **2014**, *2*, 7288–7294. [CrossRef]
79. Ju, H.; Kim, J. Transparent and Hybrid Multilayer Films with Improved Thermoelectric Performance by Chalcogenide-Interlayer-Induced Transport Enhancement. *ACS Appl. Mater. Interfaces* **2019**, *11*, 35354–35361. [CrossRef]
80. Weng, D.; Xu, F.; Li, X.; Li, S.; Li, Y.; Sun, J. Polymeric Complex-Based Transparent and Healable Ionogels with High Mechanical Strength and Ionic Conductivity as Reliable Strain Sensors. *ACS Appl. Mater. Interfaces* **2020**, *12*, 57477–57485. [CrossRef] [PubMed]
81. Lan, J.; Li, Y.; Yan, B.; Yin, C.; Ran, R.; Shi, L.-Y. Transparent Stretchable Dual-Network Ionogel with Temperature Tolerance for High-Performance Flexible Strain Sensors. *ACS Appl. Mater. Interfaces* **2020**, *12*, 37597–37606. [CrossRef] [PubMed]
82. Wang, Z.; Zhang, J.; Liu, J.; Hao, S.; Song, H.; Zhang, J. 3D Printable, Highly Stretchable, Superior Stable Ionogels Based on Poly(ionic liquid) with Hyperbranched Polymers as Macro-cross-linkers for High-Performance Strain Sensors. *ACS Appl. Mater. Interfaces* **2021**, *13*, 5614–5624. [CrossRef] [PubMed]

83. Son, J.S.; Park, K.; Han, M.-K.; Kang, C.; Park, S.-G.; Kim, J.-H.; Kim, W.; Kim, S.-J.; Hyeon, T. Large-Scale Synthesis and Characterization of the Size-Dependent Thermoelectric Properties of Uniformly Sized Bismuth Nanocrystals. *Angew. Chem. Int. Ed. Engl.* **2011**, *50*, 1363–1366. [CrossRef] [PubMed]
84. Kim, S.J.; We, J.H.; Cho, B.J. A wearable thermoelectric generator fabricated on a glass fabric. *Energy Environ. Sci.* **2014**, *7*, 1959–1965. [CrossRef]
85. Chen, B.; Das, S.R.; Zheng, W.; Zhu, B.; Xu, B.; Hong, S.; Sun, C.; Wang, X.; Wu, Y.; Claussen, J.C. Inkjet Printing of Single-Crystalline Bi2Te3 Thermoelectric Nanowire Networks. *Adv. Electron. Mater.* **2017**, *3*, 1600524. [CrossRef]
86. Matsuo, H.; Yoshitoku, K.; Saito, M.; Takahashi, H.; Terasaki, I.; Homma, T. Fabrication of ZnO-Based Thermoelectric Micro-Devices by Electrodeposition. *J. Electrochem. Soc.* **2018**, *165*, D417–D422. [CrossRef]
87. Klochko, N.; Klepikova, K.; Kopach, V.; Tyukhov, I.; Zhadan, D.; Khrypunov, G.; Petrushenko, S.; Dukarov, S.; Lyubov, V.; Kirichenko, M. Semitransparent p-CuI and n-ZnO thin films prepared by low temperature solution growth for thermoelectric conversion of near-infrared solar light. *Sol. Energy* **2018**, *171*, 704–715. [CrossRef]
88. Kaushik, N.; Saravanakumar, P.; Dhanasekhar, S.; Saminathan, R.; Rinawa, M.L.; Subbiah, R.; Sharma, R.; Kumar, P.M. Thermal analysis of a double-glazing window using a Nano-Disbanded Phase Changing Material (NDPCM). *Mater. Today Proc.* **2022**, *62*, 1702–1707. [CrossRef]
89. Ma, L.; Zhang, X.; Li, D.; Arıcı, M.; Yıldız, Ç.; Li, Q.; Zhang, S.; Jiang, W. Influence of sunspace on energy consumption of rural residential buildings. *Sol. Energy* **2020**, *211*, 336–344. [CrossRef]
90. Shemelin, V.; Matuska, T.; Sourek, B.; Jirka, V. Energy savings potential from prismatic glass structure. In Proceedings of the 11th International Conference on Environmental Science and Development, Barcelona, Spain, 10–12 February 2020; EDP Sciences: Paris, France, 2020; p. 06004. [CrossRef]
91. Katsura, T.; Memon, S.; Radwan, A.; Nakamura, M.; Nagano, K. Thermal performance analysis of a new structured-core translucent vacuum insulation panel in comparison to vacuum glazing: Experimental and theoretically validated analyses. *Sol. Energy* **2020**, *199*, 326–346. [CrossRef]
92. Ghosh, A.; Norton, B.; Duffy, A. Measured thermal & daylight performance of an evacuated glazing using an outdoor test cell. *Appl. Energy* **2016**, *177*, 196–203. [CrossRef]
93. Tom, M.S.; Richard, E.C.; Fredric, A.B.; Dariush, K.A. Edge Conduction in Vacuum Glazing. In Proceedings of the Thermal Performance of the Exterior Envelopes of Buildings VI Conference, Clearwater Beach, FL, USA, 4–8 December 1995. [CrossRef]
94. Mandal, C.; Donthula, S.; Far, H.M.; Saeed, A.M.; Sotiriou-Leventis, C.; Leventis, N. Transparent, mechanically strong, thermally insulating cross-linked silica aerogels for energy-efficient windows. *J. Sol-Gel Sci. Technol.* **2019**, *92*, 84–100. [CrossRef]
95. Buratti, C.; Belloni, E.; Merli, F.; Zinzi, M. Aerogel glazing systems for building applications: A review. *Energy Build.* **2021**, *231*, 110587. [CrossRef]
96. Ghosh, A.; Norton, B. Advances in switchable and highly insulating autonomous (self-powered) glazing systems for adaptive low energy buildings. *Renew. Energy* **2018**, *126*, 1003–1031. [CrossRef]
97. Cuce, E.; Riffat, S.B. A state-of-the-art review on innovative glazing technologies. *Renew. Sustain. Energy Rev.* **2015**, *41*, 695–714. [CrossRef]
98. Baetens, R.; Jelle, B.P.; Gustavsen, A. Properties, requirements and possibilities of smart windows for dynamic daylight and solar energy control in buildings: A state-of-the-art review. *Sol. Energy Mater. Sol. Cells* **2010**, *94*, 87–105. [CrossRef]
99. Tällberg, R.; Jelle, B.P.; Loonen, R.; Gao, T.; Hamdy, M. Comparison of the energy saving potential of adaptive and controllable smart windows: A state-of-the-art review and simulation studies of thermochromic, photochromic and electrochromic technologies. *Sol. Energy Mater. Sol. Cells* **2019**, *200*, 109828. [CrossRef]
100. Arnesano, M.; Pandarese, G.; Martarelli, M.; Naspi, F.; Gurunatha, K.L.; Sol, C.; Portnoi, M.; Ramirez, F.V.; Parkin, I.P.; Papakonstantinou, I.; et al. Optimization of the thermochromic glazing design for curtain wall buildings based on experimental measurements and dynamic simulation. *Sol. Energy* **2021**, *216*, 14–25. [CrossRef]
101. Lei, Q.; Wang, L.; Xie, H.; Yu, W. Active-passive dual-control smart window with thermochromic synergistic fluidic glass for building energy efficiency. *Build. Environ.* **2022**, *222*, 109407. [CrossRef]
102. Aburas, M.; Soebarto, V.; Williamson, T.; Liang, R.; Ebendorff-Heidepriem, H.; Wu, Y. Thermochromic smart window technologies for building application: A review. *Appl. Energy* **2019**, *255*, 113522. [CrossRef]
103. Marchwiński, J. Study of electrochromic (EC) and gasochromic (GC) glazing for buildings in aspect of energy efficiency. *Archit. Civ. Eng. Environ.* **2021**, *14*, 27–38. [CrossRef]
104. Roy, A.; Mallick, T.K.; Tahir, A.A. An optimal climate-adaptable hydrogel-filled smart window for the energy-saving built environment. *J. Mater. Chem. C* **2022**, *10*(41), 15474–15482. [CrossRef]
105. Zhou, Y.; Fan, F.; Liu, Y.; Zhao, S.; Xu, Q.; Wang, S.; Luo, D.; Long, Y. Unconventional smart windows: Materials, structures and designs. *Nano Energy* **2021**, *90*, 106613. [CrossRef]
106. Khaled, K.; Berardi, U. Current and future coating technologies for architectural glazing applications. *Energy Build.* **2021**, *244*, 111022. [CrossRef]
107. Zhou, Y.; Dong, X.; Mi, Y.; Fan, F.; Xu, Q.; Zhao, H.; Wang, S.; Long, Y. Hydrogel smart windows. *J. Mater. Chem. A* **2020**, *8*, 10007–10025. [CrossRef]
108. Bronnikov, S.; Kostromin, S.; Zuev, V. Polymer-dispersed liquid crystals: Progress in preparation, investigation, and application. *J. Macromol. Sci. Phys. Part B* **2013**, *52*, 1718–1735. [CrossRef]

109. Saeed, M.H.; Zhang, S.; Cao, Y.; Zhou, L.; Hu, J.; Muhammad, I.; Xiao, J.; Zhang, L.; Yang, H. Recent advances in the polymer dispersed liquid crystal composite and its applications. *Molecules* **2020**, *25*, 5510. [CrossRef]
110. Lami, M.; Al-naemi, F.; Alrashidi, H.; Issa, W. Quantifying of Vision through Polymer Dispersed Liquid Crystal Double-Glazed Window. *Energies* **2022**, *15*, 3196. [CrossRef]
111. Karimov, K.S.; Fatima, N.; Qasuria, T.; Siddiqui, K.; Bashir, M.; Alharbi, H.; Alharth, N.; Al-Harthi, Y.; Amin, N.; Akhtaruzzaman, M. Innovative semitransparent photo-thermoelectric cells based on bismuth antimony telluride alloy. *J. Alloys. Compd.* **2020**, *816*, 152593. [CrossRef]
112. Yang, C.; Souchay, D.; Kneiß, M.; Bogner, M.; Wei, H.; Lorenz, M.; Oeckler, O.; Benstetter, G.; Fu, Y.Q.; Grundmann, M. Transparent flexible thermoelectric material based on non-toxic earth-abundant p-type copper iodide thin film. *Nat. Commun.* **2017**, *8*, 1–7. [CrossRef] [PubMed]
113. Wang, X.; Suwardi, A.; Lim, S.L.; Wei, F.; Xu, J. Transparent flexible thin-film p–n junction thermoelectric module. *npj Flex. Electron.* **2020**, *4*, 1–9. [CrossRef]
114. Zhang, Q.; Huang, A.; Ai, X.; Liao, J.; Song, Q.; Reith, H.; Cao, X.; Fang, Y.; Schierning, G.; Nielsch, K. Transparent Power-Generating Windows Based on Solar-Thermal-Electric Conversion. *Adv. Energy Mater.* **2021**, *11*, 2101213. [CrossRef]
115. He, S.; Li, Y.; Liu, L.; Jiang, Y.; Feng, J.; Zhu, W.; Zhang, J.; Dong, Z.; Deng, Y.; Luo, J. Semiconductor glass with superior flexibility and high room temperature thermoelectric performance. *Sci. Adv.* **2020**, *6*, eaaz8423. [CrossRef]
116. Van Dessel, S.; Foubert, B. Active thermal insulators: Finite elements modeling and parametric study of thermoelectric modules integrated into a double pane glazing system. *Energy Build.* **2010**, *42*, 1156–1164. [CrossRef]
117. He, M.; Lin, Y.-J.; Chiu, C.-M.; Yang, W.; Zhang, B.; Yun, D.; Xie, Y.; Lin, Z.-H. A flexible photo-thermoelectric nanogenerator based on MoS2/PU photothermal layer for infrared light harvesting. *Nano Energy* **2018**, *49*, 588–595. [CrossRef]
118. Norouzi, M.; Kolahdouz, M.; Ebrahimi, P.; Ganjian, M.; Soleimanzadeh, R.; Narimani, K.; Radamson, H. Thermoelectric energy harvesting using array of vertically aligned Al-doped ZnO nanorods. *Thin Solid Film.* **2016**, *619*, 41–47. [CrossRef]
119. Ito, Y.; Mizoshiri, M.; Mikami, M.; Kondo, T.; Sakurai, J.; Hata, S. Fabrication of thin-film thermoelectric generators with ball lenses for conversion of near-infrared solar light. *Jpn. J. Appl. Phys.* **2017**, *56*, 06GN06. [CrossRef]
120. Murmu, P.P.; Shettigar, A.; Chong, S.V.; Liu, Z.; Goodacre, D.; Jovic, V.; Mori, T.; Smith, K.E.; Kennedy, J. Role of phase separation in nanocomposite indium-tin-oxide films for transparent thermoelectric applications. *J. Mater.* **2021**, *7*, 612–620. [CrossRef]
121. Mokaripoor, E.; Bagheri-Mohagheghi, M.-M. Effect of very low to high Sb-doping on the structural, electrical, photo-conductive and thermoelectric properties of fluorine-doped SnO2 (FTO) thin films prepared by spray pyrolysis technique. *J. Mater. Sci. Mater. Electron.* **2016**, *27*, 2305–2314. [CrossRef]
122. Kang, S.; Fu, Y.; Gu, H.; Lin, C. Chalcogenide glass for thermoelectric application. *J. Non-Cryst. Solids: X* **2022**, *15*, 100111. [CrossRef]
123. Inayat, S.B.; Rader, K.R.; Hussain, M.M. Nano-materials enabled thermoelectricity from window glasses. *Sci. Rep.* **2012**, *2*, 1–7. [CrossRef] [PubMed]
124. Indab, M.B.L.; Ng, J.A.T.; Reyeg, L.A.F.P.; Tuppil, R.A.G.; Umali, R.; Manuel, M.C.E.; Cruz, J.C.D.; Tud, R.C. Design, Fabrication, and Testing of Thermoelectric Generators Integrated on a Residential Window Frame. In Proceedings of the 2021 IEEE International Conference on Automatic Control & Intelligent Systems (I2CACIS), Shah Alam, Malaysia, 26 June 2021; pp. 197–202. [CrossRef]
125. Inayat, S.B.; Hussain, M.M. Power generation from thermoelectric system-embedded Plexiglas for green building technology. *Appl. Nanosci.* **2013**, *3*, 335–342. [CrossRef]
126. Energy Bills Support Factsheet. Available online: https://www.gov.uk/government/publications/energy-bills-support/energy-bills-support-factsheet-8-september-2022 (accessed on 11 November 2022).